

**Danko, V.A., Indutnyi, I.Z., Ushenin, Yu.V., Lytvyn, P.M.,
Mynko, V.I., Shepeliavyi, P.E., Lukaniuk, M.V., Korchovy, A.A., and Khristosenko, R.V.**

Lashkariov Institute of Semiconductor Physics, the NAS of Ukraine, 41, Nauky Ave., 03028, Kyiv, Ukraine,
tel. +380 44 525 6342, indutnyi@isp.kiev.ua

DEVELOPMENT OF TECHNOLOGY FOR SENSOR CHIP PRODUCTION WITH ENHANCED SENSITIVITY AND IMPROVED PHYSICAL AND MECHANICAL CHARACTERISTICS FOR OPTICAL SENSORS BASED ON SURFACE PLASMON RESONANCE



An innovative project on the development of a method for manufacturing sensor chips with enhanced sensitivity for biosensors based on surface plasmon resonance (SPR) operating in the Kretschmann scheme has been completed. An increase in sensitivity of such sensor has been achieved by forming high-frequency periodic grating on the sensor chip surface using the interference photolithography technique. All processes have been optimized. A pilot sample of modernized SPR refractometer as well as a pilot batch of nanostructured sensor chips with spatial frequencies up to 3400 mm^{-1} have been manufactured and tested. The use of nanostructured chips has resulted in a 4.7-time increase in the SPR refractometer sensitivity.

Key words: surface plasmon resonance, biosensors, interference lithography, and vacuum chalcogenide photoresists.

Optical sensors based on surface plasmon resonance (SPR) are widely used in biology, medicine, ecology, food, chemical, and pharmaceutical industries, agriculture, etc. [1–5]. However, the sensitivity of these biosensors gets lower as the size of studied biological molecules decreases. In particular, modern SPR-based biosensors are usually insufficiently sensitive to detect the interaction of proteins with small ligand molecules [6].

As previous theoretical and experimental studies of French authors [7, 8] have shown, one of the ways to increase the sensitivity of SPR based biosensor in the Kretschmann scheme is the formation of a periodic lattice on the surface of metal layer of sensor chip. Periodic nanostructures are formed

using advanced lithographic technologies: electron beam or ion beam lithography [9, 10], nanospheric lithography [11], nano-stamping [12], optical lithography in the far ultraviolet region [13] and other fairly costly processes. As a result, their price is too high, which makes questionable their widespread use.

At the same time, interference lithography (IL) is cheaper and technologically simpler, which can be used for the formation of ordered metallic nanostructures [14, 15]. In previous studies, IL has been shown to be a promising technology for the formation of one- and two-dimensional submicron periodic structures on the surface of metallic films, semiconductors, and insulators using a high-resolution vacuum photoresist based on chalcogenide glass (CG) [16, 17].

Therefore, the main objective of innovation project was to develop and to optimize interfer-

ence photolithography technological processes using vacuum photoresists for manufacturing sensor chips with high sensitivity and improved physical and mechanical properties for SPR-based optical sensors.

DESIGN AND SETTING UP OF OPTICAL SCHEMES AND OPTIMIZATION OF PROCESSES FOR MANUFACTURING HIGH-FREQUENCY PLASMON STRUCTURES

Theoretical calculations have shown that in order to effectively increase sensitivity of sensor chips, the surface of gold plasmon-generating layer should be nanostructured with a grating period of 3000 to 3400 nm⁻¹. To produce such high-frequency structures, it is necessary to optimize the processes for vacuum application of gold and vacuum chalcogenide photoresist coating, exposure, post-exposure treatment, and etch of plasmon-generating layer.

The IL scheme is shown in Fig. 1. A multilayer structure (Fig. 1, *a*) consisting of substrate (1), working layer of gold (2), and photoresist layer (3) are exposed to interference field from two coherent laser beams (4). The interference pattern period (Λ) is determined by the formula: $\Lambda = (\lambda/2n)\sin(\theta/2)$, where λ is light wavelength in vacuum, n is refractive index of medium where interference pattern is formed, and θ is beam convergence angle.

The exposure is followed by controlled selective etch of inorganic chalcogenide photoresist and formation of a mask consisting of parallel lines (Fig. 1, *b*). Further, the working (plasmon-generating gold) layer is etched (Fig. 1, *c*). The mask having been removed, a diffraction structure remains on the working layer surface (Fig. 1, *d*).

The optimum conditions for vacuum application of gold using the IL technique have been established to be as follows. The samples are prepared by consecutive thermal evaporation in vacuum (2×10^{-3} Pa) and condensation on the substrates of 3 nm thick chromium (Cr) adhesive layer, 40–50 nm thick metal (Au) and 50–100 nm thick chalcogenide photoresist layers (depend-

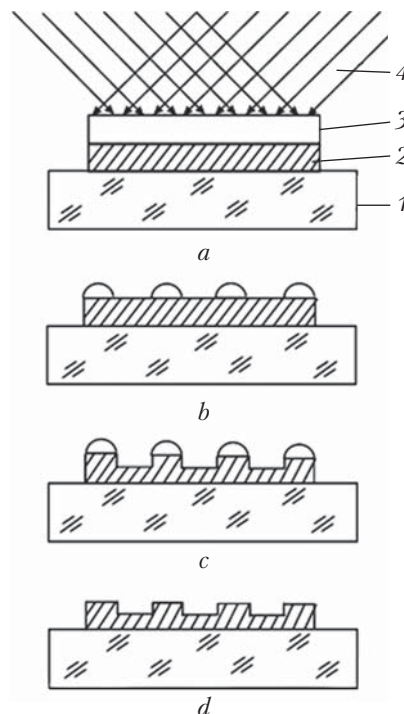


Fig. 1. Scheme of interference lithography process

ing on the spatial frequency of nanostructures). Polished plates of F1 glass ($n = 1.615$, dimensions $20 \times 20 \times 1$ mm) are used as substrates. The thickness is controlled by a quartz thickness meter (KIT-1) during the film application and by a microinterferometer MII-4 and an ellipsometer LEF-3M after the deposition.

The interference structures on chalcogenide photoresist films are recorded using an interference pattern from helium-cadmium laser ($\lambda = 441.6$ nm) radiation with a given spatial frequency. The optimal exposure when recording high-frequency interference masks is 0.2–0.5 J/cm².

After exposure, using selective etching solution based on anhydrous ethylenediamine solution, a lithographic mask is formed, through which the metal film is etched.

The etching of photoresist and plasmon-generating layers is controlled in situ by recording non-photoactive long-wave light diffracted from the relief structure formed during the etching. After removal of residual photoresist in alkali



Fig. 2. Optical scheme of recording interference pattern on chips for SPR refractometer

solution, washing and drying, a metallic periodic structure is obtained.

Fig. 2 shows a photo of an optical scheme assembled on a vibration-resistant plate in a room with controlled temperature and humidity.

PRODUCTION OF PILOT SAMPLES AND STUDY OF THEIR PROPERTIES

After interference lithography technique optimization, thirty pilot dual-channel gold chips with various lattice parameters (relief depth, slit between the nanowires, period) have been made. The periodic structure was formed only on the one side of the chip, the other side remaining coated with unstructured gold film. The samples were prepared for comparative study on dual-channel device. The researchers used upgraded dual-channel SPR-refractometer PLASMON-71M in the Kretschmann configuration developed at the Lashkarev Institute of Semiconductor Physics of the NAS of Ukraine with a semiconductor laser having a wavelength of 850 nm as radiation source.

The lattice spatial frequency was selected based on the condition of proximity to the Bragg reflection. The theoretical modeling in [7] was performed for sinusoidal gratings with a small depth of relief. In this case, it is possible to estimate approximate Bragg grating constant (Λ_B)

using the formula [18]:

$$\Lambda_B = 0,5\lambda_0 [(\varepsilon_{mr} + \varepsilon_D)/\varepsilon_{mr}\varepsilon_D]^{1/2} / \cos\varphi, \quad (1)$$

where λ_0 is light wavelength in vacuum, φ is azimuth angle that is the angle between the incident plane of probe beam and the grating wave vector perpendicular to grating lines, $\varepsilon_D = n^2$ is dielectric constant (n is refractive index, glycerin aqueous solution), and ε_{mr} is real part of metal dielectric constant (in this case, gold). For Au–water interface (water refractive index at 20 °C is 1.333) at an excitation wavelength of 850 nm the condition of Bragg resonance corresponds to a grating period of about 309 nm (spatial frequency $\nu = 3240$ lines/mm). The dielectric permeability of gold is taken from [19]. As the refractive index of medium interfacing gold increases the resonance condition is met at lesser grating periods. For instance, for glycerin with $n = 1.474$ at 20 °C the Bragg resonance corresponds to a period of 277 nm ($\nu = 3610$ lines/mm). Proceeding from the above estimates, samples with spatial frequencies of periodical nanorelief taken within the mentioned range have been manufactured using the IL method.

Fig. 3 shows photos of the first series of dual-channel chip prototypes, where polychromatic light falls perpendicularly to grating lines (*a*) and in parallel to the lines (*b*). In the first case, the observed spectra on sample surface appear as a result of light diffraction on gratings, whereas in the second case, intensity of reflection on gratings with different relief depth differs.

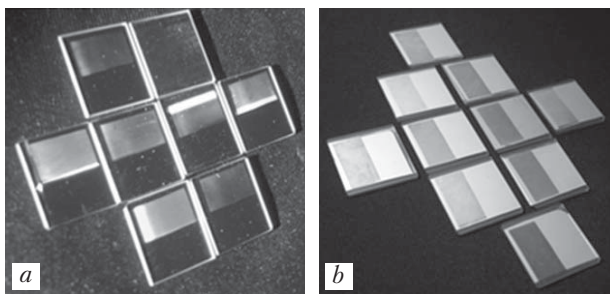


Fig. 3. Dual-channel chip prototypes: *a* – light falls perpendicular to the grating lines, *b* – light falls in parallel to the grating lines

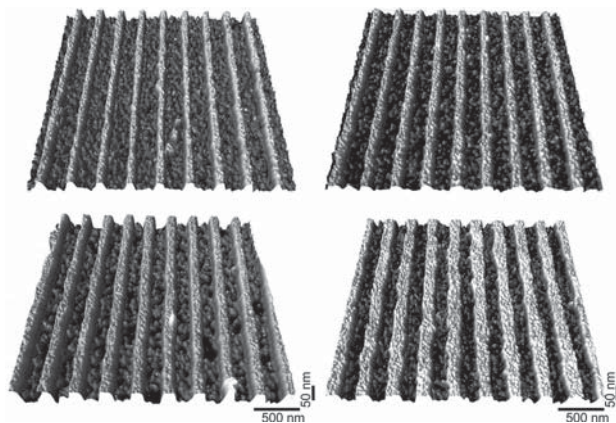


Fig. 4. AFM images of gratings with a period of 296.6 ± 0.5 nm and different depth of relief



Fig. 5. AFM images of Au-chips with a period of 296.6 ± 0.5 nm and an average relief depth of 13.5 ± 2 nm (a) and 21.0 ± 2 nm (b)

Atomic force microscope (AFM) *Dimension 3000 Scanning Probe Microscope (Digital Instruments Inc., Tonawanda, NY, USA)* was used to determine the shape of relief elements of periodic structure and their dimensions. The spatial frequency of gratings was measured using an optical stand based on G5M goniometer with an accuracy of ± 5 lines/mm.

Fig. 4 shows AFM images of a relief of samples with the same grating period, but with different line widths varying from 90 to 150 nm.

The PLAZMON-71M refractometer enables to measure angular dependences of internal reflection intensity $R(\theta)$ for the gold film and to determine the position of reflection minimum (θ_{\min}) that corresponds to the excitement of surface plasmons on the gold-medium interface. θ_{\min} is rather sensitive to varying refractive index n of the medium near the surface of gold film, which enables recording the processes resulting in very small variations of n in this area. To determine the structure sensor sensitivity, i.e. the influence of

medium refractive index on the resonance minimum shift, a glycerin aqueous solution of various concentrations was introduced into a dual-channel flow-through cell located above the sample studied in such a way as the fluid interfaces the structure, with one channel corresponding to the reference gold film and the other one to the nanostructured film (with a surface relief formed as grating).

The sensitivity of structured chips has been studied in detail on the samples whose AFM images are shown in Fig. 5. These gratings have the same period of 296.6 ± 0.5 nm ($\nu = 3372$ mm⁻¹), but the golden film is etched through a photoresist mask for different time, which results in a different depth of relief: 13.5 ± 2 nm (a) and 21.0 ± 2 nm (b).

The dependence of θ_{\min} on the medium refractive index for these gratings is featured in Fig. 6. Curve 1 on all diagrams shows $\theta_{\min}(n)$ dependence for standard Au-sensor with an unstructured surface. It can be seen that as n increases, θ_{\min} also grows monotonously, with the slope angle ($\Delta\theta_{\min}$ to Δn ratio) being almost constant over the entire studied range of n and equal to about 100 deg./RIU (where RIU is refractive index unit). The ratio of the minimum position shift $\Delta\theta_{\min}$ to the corresponding change in the refractive index Δn characterizes the method sensitivity to varying medium refractive index n near the surface of the metal film.

Curve 2 in Fig. 6 a corresponds to a sensor with a structured surface and a small depth of relief (13.5 nm). The chip is oriented in such a way that the incident plane of probe beam is perpendicular to the lines. For the structured chip, the $\theta_{\min}(n)$ dependence is nonlinear: when approximating the Bragg resonance condition, the slope of this dependence decreases significantly as compared with the standard chip, and further, there is a section of high sensitivity within the range of refractive index variation $\Delta n = 0.009$.

This range is highlighted by two vertical dashed lines in Fig. 6. Within the high sensitivity range, the experimental points are approximated with

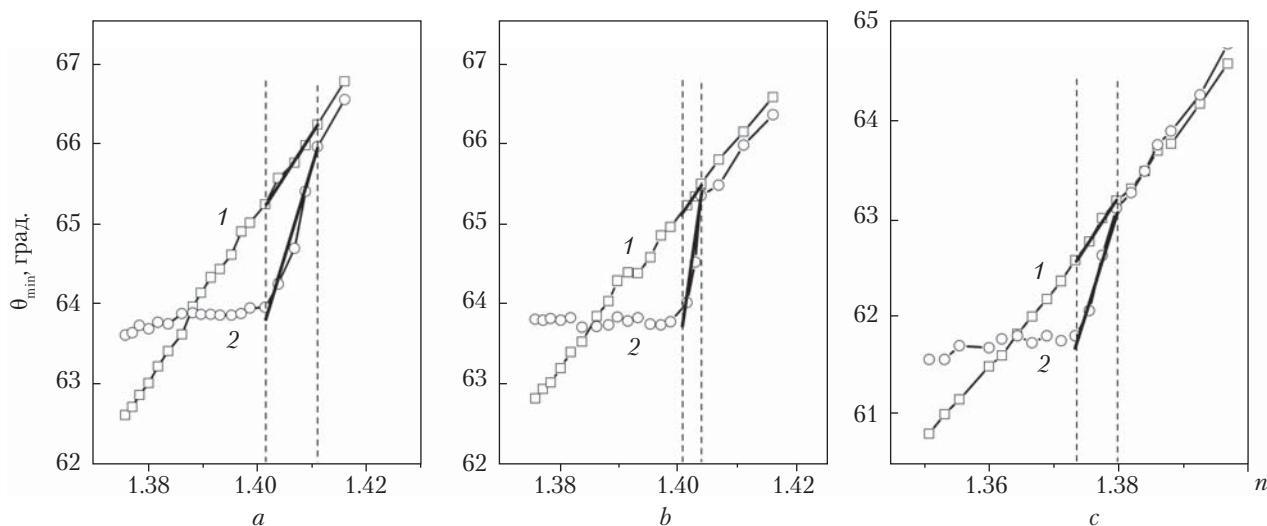


Fig. 6. Dependence of SPR resonance position θ_{\min} on refractive index n for the standard Au-chip with a smooth surface (curve 1 (a), (b), and (c)) and Au-gratings with a period of 296.6 ± 0.5 nm and a relief depth of 13.5 ± 2 nm (curve 2 (a)) and 21.0 ± 2 nm (curve 2 (b)). Curve 2 (c) shows $\theta_{\min}(n)$ dependence for Au-grating with a period of 302.0 ± 0.5 nm and an average relief depth of 17.5 ± 2 nm

straight line segments. For the test sample the ratio of slopes of these segments, that is, the ratio of sensitivity of the structured and the standard chips is 2.4.

Fig. 6, *b* (curve 2) shows the $\theta_{\min}(n)$ dependences for structured sample with a greater depth of grating relief (21 nm). The range of increased steepness, which is marked by vertical dashed lines, is also significantly narrowed for this sample ($\Delta n = 0.0031$) as compared with the chips having a lower depth of relief, but the magnitude of steepness increases essentially. The ratio of segment slopes, which approximates the experimental points for the standard and the structured chips in the high sensitivity range, is 4.4. For this batch of samples (Fig. 5), the sensitivity increases from ~ 100 deg/RIU for the standard chips up to 260 deg/RIU for the structured chips with a lower depth of relief and up to 480 deg/RIU for the chips with a greater one. However, for all samples studied, the general pattern has been observed: as the relief deepens, Δn (the width of refractive index range where sensitivity grows) gets narrowed, with the sensitivity increasing within this range.

An increase in sensitivity of structured SPR sensor chips within a limited refractive index variation range is consistent with the results of theoretical studies that suggested an increase in sensitivity within the range of Δn less than 0.01 [7]. The biochemical processes studied with the use of SPR refractometer are often accompanied with deposition of biomolecule monolayers with very small variations of refractive index. The refractive resolution of *Plasmon-71M* refractometer being $\Delta n = 5 \cdot 10^{-6}$ RIU, the operation range Δn less than 0.01 RIU may be sufficient for such measurements (it can embrace several hundred experimental points).

In addition, the operation range with enhanced sensitivity of sensor can approach the refractive index of medium studied by changing the grating's spatial frequency. Fig. 6, *c* (curve 2) featured $\theta_{\min}(n)$ dependence for Au-grating with a period of 302.0 ± 0.5 nm and an average depth of relief of 17.5 ± 2 nm. The range of Δn with enhanced sensitivity shifts by 0.026–0.030 RIU towards lower n as compared with the results for gratings with a period of 296.6 nm (Figs. 6, *a*, *b*, curves 2). Having solved the equation (1) with

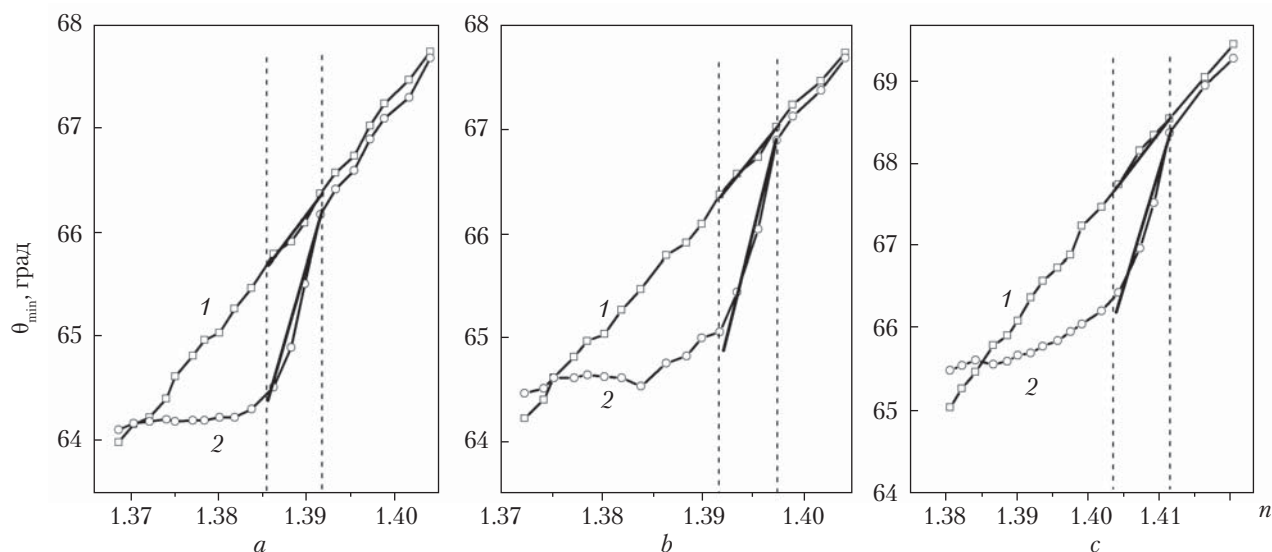


Fig. 7. Dependence of SPR resonance position θ_{\min} on refractive index n for the standard Au-chip (curve 1) and Au-grating with a period of 296.6 ± 0.5 nm and a relief depth of 13.5 ± 2 nm (curve 2) coated with a 4 nm thick chromium layer: *a* – incidence plane of probe beam is perpendicular to the grating lines (azimuth angle $\varphi = 0$), *b* – $\varphi = 5.7^\circ$, and *c* – $\varphi = 10^\circ$

respect to n , one can estimate a shift in resonant refractive index resulted from increase in the grating's period from 296.6 nm to 302.0 nm. The obtained shift in the position of operation range is 0.024 RIU at $\varphi = 0$ that is in good agreement (especially for such a simplified dependence) with given experimental data.

However, this way of approximating the operation range to the medium refractive index is quite costly, since it is necessary to make a set of structured chips with different spatial frequencies. On the other hand, the position of operation range can also be changed by modifying the chip sur-

face. Fig. 7 *a* shows the dependences of minimum SPR position on the refractive index of the studied solution for standard Au-sensor (curve 1) and for Au-grating with a depth of 13.5 ± 2 nm (curve 2) coated with a 4 nm chromium layer. This islet chromium layer is deposited by the method of thermal evaporation in vacuum. Such a modification of the chip surface leads to a shift in the operation range position by 0.018 RIU towards lower n as compared with the unmodified analogue chip (Fig. 6, *a*, curve 2).

Consequently, instead of making diffraction gratings with different frequency, a thin layer of metal or dielectric can be applied to the chip surface. This process is much cheaper than making the gratings. However, this chip modification is irreversible and leads to changing conditions of immobilization of biomolecule monolayers on the chip surface.

The most convenient way of approximating the operation range position to the refractive index of the studied medium may be to vary the azimuthal angle. Fig. 7, *b* shows $\theta_{\min}(n)$ dependencies for the same dual-channel chip as in Fig. 7, *a*, but the sample was fixed in the SPR refractometer in such a

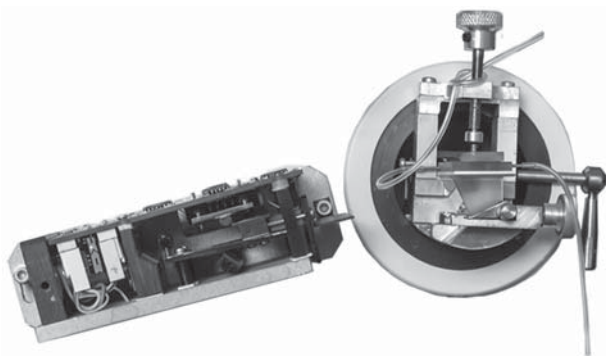


Fig. 8. PLASMON-71M biosensor refractometer

way that the incident plane of probe beam was oriented at 5.7° relative to the grating wave vector ($\varphi = 5.7^\circ$). Fig. 7, c features results for the same sample at $\varphi = 10^\circ$. It should be noted that the operation range shifts towards higher refractive index by 0.0056 RIU at $\varphi = 5.7^\circ$ and by 0.0184 RIU at $\varphi = 10^\circ$, as the azimuth angle increases. Calculations by formula (1) have given shifts of 0.006 RIU and 0.020 RIU, respectively, which are in good agreement with the experimental data.

These results show that at small variations of the azimuthal angle the SPR measurements using the high sensitivity range can be done within a wide range of refractive index variations on one nanostructured chip.

The use of structured chips with high sensitivity also requires some upgrade of existing refractometer based on surface plasmon resonance. In particular, as the above mentioned research results have shown, in order to cover all required range of refractive index by the range of enhanced sensitivity of structured chip, the device design shall allow the chip to rotate azimuthally within 10 degrees. In order to solve this problem in the project framework, a design has been developed and a prototype model of upgraded SPR-refractometer *PLASMON-71M* has been made (Fig. 8). The small refractometer modified for measurements using nanostructured chips with high sensitivity is configured in such a way as to enable varying the chip orientation within 10 degrees in the azimuthal direction (the rotation around the axis that is perpendicular to the sample plane and passes through the point of light incidence onto a plasmon-supporting film).

The specifications of small multi-purpose refractometer are shown in Table. These parameters have been obtained from the acceptance tests of model sample.

CONCLUSIONS

The processes of interference lithography with the use of vacuum photoresists for the manufacture of nanostructured sensory chips with spatial frequencies up to 3400 lines/mm, enhanced sen-

**Specifications
of *PLASMON-71M* Refractometer**

Parameter	Value
Range of refractive index measurement	1.0–1.45
Resolution of refractometer for refractive index measurements	$5 \cdot 10^{-6}$
Incidence angle resolution	10 angular seconds
Maximum scanning angle	17°
Maximum azimuth rotation angle	10°
SPR full curve measurement time, sec	≤ 3
Minimum time per a single measurement: Measurement in SPR-curve mode, sec	2.5
Number of optical channels	2
Radiation source: GaAs semiconductor laser, wavelength, nm	$\lambda = 850 \text{ nm}$
Connection to PC	USB
Software	Plas 7XE

sitivity, and improved physical and mechanical properties for optical sensors based on surface plasmon resonance have been optimized.

A method for adjusting the operation range of nanostructured sensor chip to the refractive index of the studied medium by chip azimuthal rotation has been developed. To this end, the SPR refractometer has been upgraded.

A prototype SPR refractometer and an experimental batch of nanostructured sensor chips have been manufactured and tested. The results of sensor sensitivity measurements have confirmed the theoretical suggestion that the sensitivity of SPR-biosensors can be enhanced by forming a grating with corresponding period and relief depth on the chip working surface. The multiplicity of sensitivity increase and the range of refractive index variations in the medium where this increase is observed have been established to depend on the relief depth. As the relief depth increases, the operation range gets narrower, and the multiplicity of increase in sensitivity grows. The SPR refractometer sensitiv-

ity increases 4.7 times due to the use of nanostructured chips.

The main advantage of the project deliverables is enhancement of SPR-biosensor sensitivity. The cost of nanostructured chips will be UAH 300–350 per unit depending on its characteristics. The minimum price for foreign counterpart with standard unstructured gold layers is EUR 40 per unit.

REFERENCES

- Nylander C., Liedberg B., Lind T. Gas detection by means of surface plasmon resonance. *Sens. Actuators*. 1982. V. 3. P. 79–88.
- Schmitt H.-M., Brecht A., Piehler J., Gauglitz G. An integrated system for optical biomolecular interaction analysis. *Biosensors and Bioelectronics*. 1997. 12 (8): 809–816.
- Huang L., Reekmans G., Saerens D., Friedt J.-M., Frederix F., Francis L., Muyldermans S., Campitelli A., Van Hoof C. Prostate-specific antigen immunosensing based on mixed self-assembled monolayers, camel antibodies and colloidal gold enhanced sandwich assays. *Biosensors & Bioelectronics*. 2005. 21 (3): 483–490.
- Mauriz E., Calle A., Manclús J.J., Montoya A., Lechuga L.M. Multi-analyte SPR immunoassays for environmental biosensing of pesticides. *Analytical and Bioanalytical Chemistry*. 2007. 387 (4): 1449–1458.
- Patel P.D. Overview of affinity biosensors in food analysis. *Journal of AOAC International*. 2006. 89 (3): 805–818.
- Patrick Englebienne, Anne Van Hoonacker, Michel Verhas. Surface plasmon resonance: principles, methods and applications in biomedical sciences. *Spectroscopy*. 2003. 17 (2, 3): 255–273.
- Alleyne C.J., Kirk A.G., McPhedran R.C., Nicorovici N.-A.P. and Maystre D. Enhanced SPR sensitivity using periodic metallic structures. *Opt. Express*. 2007. V. 15. P. 8163–8169.
- Dan'ko V.A., Dorozinsky G.V., Indutnyi I.Z., Myn'ko V.I., Ushenin Yu.V., Shepeliavyy P.E., Lukaniuk M.V., Korchovyy A.A., Khrystosenko R.V. Nanopatterning Au chips for SPR refractometer by using interference lithography and chalcogenide photoresist. *Semiconductor Physics, Quantum Electronics & Optoelectronics*. 2015. 18 (4): 438.
- Cattoni A., Cambril E., Decanini D., Faini G., Haghiri-Gosnet A.M. Soft UV-NIL at 20 nm scale using flexible bi-layer stamp casted on HSQ master mold. *Microelectronic Engineering*. 2010. V. 87. P. 1015–1018.
- Fu Y., Kok N., Bryan A., Zhou W. Quasi-direct writing of diffractive structures with a focused ion beam. *Optics Express*. 2004. 12 (9): 1803.
- Zhang X.Y., Whitney A.V., Zhao J., Hicks E.M., Van Duyne R.P. Advances in contemporary nanosphere lithographic techniques. *J. Nanosci. Nanotechnol.* 2006. 6 (7): 1920–1934.
- Chuang S.Y., Chen H.L., Kuo S.S., Lai Y.H., Lee C.C. Using direct nanoimprinting to study extraordinary transmission in textured metal films. *Optics Express*. 2008. 16 (4): 2415.
- Briзуela F., Wang Y., Brewer C.A., Pedaci F., Chao W., Anderson E.H., Liu Y., Goldberg K.A., Naulleau P., Wachulak P., Marconi M.C., Attwood D.T., Rocca J.J., Menoni C.S. Microscopy of extreme ultraviolet lithography masks with 13.2 nm tabletop laser illumination. *Optics Letters*. 2009. 34 (3): 271–273.
- Alexander Arriola, Ainara Rodriguez, Noemi Perez, Txaber Tavera, Michael J. Withford, Alexander Fuerbach, Santiago M. Olaizola. Fabrication of high quality sub-micron Au gratings over large areas with pulsed laser interference lithography for SPR sensors. *Opt. Mater. Express*. 2012. 2 (11): 1571–1579.
- Vala M., Homola J. Flexible method based on four-beam interference lithography for fabrication of large areas of perfectly periodic plasmonic arrays. *Optics Express*. 2014. 22 (15): 18778.
- Indutnyi I., Min'ko V., Shepelyavyy P., Sopinsky M., Tkach V., Dan'ko V. Growth of the photonic nanostructures using interference lithography and oblique deposition in vacuum. *Optoelectronika I Poluprovodnikova Tehnika* (Ukraine). 2011. 46: 47–54.
- Dan'ko V., Indutnyi I., Min'ko M., Shepelyavyy P. Interference photolithography with the use of resists on the basis of chalcogenide glassy semiconductors. *Optoelectronics, Instrumentation and Data Processing*. 2010. 46 (5): 483–490.
- Gazzola E., Brigo L., Zacco G., Zilio P., Ruffato G., Brusatin G., Romanato F. Coupled SPP Modes on 1D Plasmonic Gratings in Conical Mounting. *Plasmonics, Springer Science+Business Media*. New York. 2013. 9 (4): 867–876.
- Johnson P. B., Christy R. W. Optical Constants of the Noble Metals. *Phys. Rev.* 1972. B 6: 4370–4379.

Received 10.05.17

*В.А. Данько, І.З. Индутний, Ю.В. Ушенін,
П.М. Литвин, В.І. Минько, П.Є. Шепелявий,
М.В. Луканюк, А.А. Корчовий, Р.В. Христосенко*

Інститут фізики напівпровідників
ім. В.Є. Лашкарьова НАН України,
просп. Науки, 41, Київ, 03028, Україна
тел. +380 44 525 5487, indutnyy@isp.kiev.ua

**РОЗРОБКА ТЕХНОЛОГІЇ ВИГОТОВЛЕННЯ
СЕНСОРНИХ ЧИПІВ З ПІДВИЩЕНОЮ
ЧУТЛИВІСТЮ ТА ПОКРАЩЕНИМИ
ФІЗИКО-МЕХАНІЧНИМИ
ХАРАКТЕРИСТИКАМИ ДЛЯ ОПТИЧНИХ
СЕНСОРІВ НА ОСНОВІ ПОВЕРХНЕВОГО
ПЛАЗМОННОГО РЕЗОНАНСУ**

Виконано інноваційний проект з розробки технологічного методу виготовлення сенсорних чипів з підвищеною чутливістю для біосенсорів на основі поверхневого плазмонного резонансу (ППР), які працюють в схемі Кречмана. Підвищення чутливості такого сенсора досягається за рахунок формування високочастотної періодичної ґратки на поверхні сенсорного чипа за допомогою інтерференційної фотолітографії. Оптимізовано технологічні процеси, виготовлено та випробувано дослідний зразок модернізованого ППР рефрактометра та експериментальну партію наноструктурованих сенсорних чипів з просторовими частотами до 3400 лін/мм. Досягнуто збільшення чутливості ППР рефрактометра у 4,7 рази за рахунок застосування наноструктурованих чипів.

Ключові слова: поверхневий плазмонний резонанс, біосенсори, інтерференційна літографія, вакуумні халькогенідні фоторезисти.

*В.А. Данько, И.З. Индутный, Ю.В. Ушенин,
П.М. Литвин, В.И. Минько, П.Е. Шепелявий,
М.В. Луканюк, А.А. Корчевой, Р.В. Христосенко*

Інститут фізики напівпровідників
ім. В.Е. Лашкарева НАН України,
просп. Науки, 41, Київ, 03028, Україна,
тел. +380 44 525 6342, indutnyy@isp.kiev.ua

**РАЗРАБОТКА ТЕХНОЛОГИИ ПРОИЗВОДСТВА
СЕНСОРНЫХ ЧИПОВ С ПОВЫШЕННОЙ
ЧУВСТВИТЕЛЬНОСТЬЮ И УЛУЧШЕННЫМИ
ФИЗИКО-МЕХАНИЧЕСКИМИ
ХАРАКТЕРИСТИКАМИ ДЛЯ ОПТИЧЕСКИХ
СЕНСОРОВ НА ОСНОВЕ ПОВЕРХНОСТНОГО
ПЛАЗМОННОГО РЕЗОНАНСА**

Выполнен инновационный проект по разработке технологического метода изготовления сенсорных чипов с повышенной чувствительностью для биосенсоров на основе поверхностного плазмонного резонанса (ППР), работающих в схеме Кречмана. Повышение чувствительности такого сенсора достигается путем формирования высокочастотной периодической решетки на поверхности сенсорного чипа с помощью интерференционной фотолитографии. Оптимизированы технологические процессы, изготовлен и испытан экспериментальный образец модернизированного ППР рефрактометра, а также экспериментальная партия наноструктурированных сенсорных чипов с пространственными частотами до 3400 лин/мм. Достигнуто увеличение чувствительности ППР рефрактометра в 4,7 раза за счет использования наноструктурированных чипов.

Ключевые слова: поверхностный плазмонный резонанс, биосенсоры, интерференционная литография, вакуумные халькогенидные фоторезисты.